

Interplay of surface preroughening, roughening, and melting in three-dimensional lattice models

E. A. Jagla^{1,*} and E. Tosatti^{1,2,3}

¹*The Abdus Salam International Centre for Theoretical Physics (ICTP), I-34014 Trieste, Italy*

²*International School for Advanced Studies (SISSA-ISAS), I-34014 Trieste, Italy*

³*Istituto Nazionale per la Fisica della Materia (INFN), Unita' SISSA, Trieste, Italy*

(Received 7 March 2000)

We elaborate upon a recently proposed surface model consisting of a domain wall induced by a twisted boundary condition in a three-dimensional N -state Potts model. The model is capable of describing simultaneously surface melting and roughening degrees of freedom and their interplay. The N different spin directions effectively describe the positional entropy, the location of the wall describes the height fluctuations, and both aspects coexist in the same system. Their interplay, known to give rise to an additional preroughening transition of the free-standing surface, is shown here to produce an adsorption phase diagram on an attractive substrate exhibiting the possibility of reentrant layering. The results provide a consistent scenario closely reminiscent of experimental results for multilayers of rare gases.

I. INTRODUCTION

There is evidence for a variety of phenomena that take place at the surface of a crystal at high temperature. One is surface melting (SM), well documented experimentally and theoretically^{1,2} to take place when the triple point temperature is approached along the solid-vapor coexistence line. SM consists of the appearance at the gas-solid interface of an intervening liquid layer whose thickness grows critically as the triple point is approached. A different class of phenomena concerns the behavior with temperature of the solid-vapor interface coordinate, the so-called surface height profile $h(x,y)$. Surface roughening (SR) is a transition where the surface height profile switches from a flat configuration at low temperatures to a rough and therefore delocalized configuration at high temperatures.³

Although these two kinds of phenomena SM and SR often tend to take place on the same crystal face and in similar temperature regimes, the theoretical equipment historically developed to describe them is quite different. SM can usefully be described, for example, by means of a phenomenological Landau-Ginzburg-type approach,¹ or by more microscopic fully three-dimensional mean-field theories,⁴⁻⁶ the latter being capable of describing the coexistence of solid, liquid, and gas at the triple point, and emphasizing precisely the configurational entropy difference of solid and liquid. However, one crucial drawback of the mean-field treatment of SM is uniformity of order parameters in each layer,⁴⁻⁶ which totally removes the possibility of height fluctuations and impedes the study of roughening. On the other hand, SR and more generally phase transitions in the height profile of crystal surfaces are usually addressed with the help of solid-on-solid (SOS) model Hamiltonians. These are lattice models where the surface is described through a height variable $h(x_{ij}, y_{ij})$, where x_{ij}, y_{ij} denote coordinates of two-dimensional (2D) lattice sites. The critical properties of SOS models at the roughening transition are usually studied with renormalization group techniques, the standard way being a mapping to a sine-Gordon Hamiltonian.⁷

A second, slightly less popular transition predicted to oc-

cur in the height profile of SOS models is the preroughening (PR) transition.⁸ This is known to occur whenever, in addition to nearest-neighbor interactions in the SOS model, there are extra terms such as longer-range interactions, with a sign that prevents the surface from becoming rough at large length scales, while still allowing for large local height fluctuations. Under these conditions, small and large scale height fluctuations may decouple, the former leading to an order-disorder PR phase transition separately from, and in fact at a lower temperature than, SR, which is driven by large scale height fluctuations. The nature of the surface in the temperature interval between PR and SR is that of a disordered flat (DOF) phase, characterized by short-range disorder, but by long-range flatness, characterized by half-integer coverage in the topmost layer.⁸⁻¹⁰ PR is predicted to be in general a nonuniversal, continuous transition, although first-order PR is expected if the ratio of the transition temperatures is sufficiently small, $T_{PR}/T_R < 1/4$.^{9,10}

The issue of the possible interplay of surface melting with roughness phenomena has not been addressed in great detail so far, mostly because of the difficulty of constructing soluble models incorporating and treating simultaneously all the degrees of freedom necessary to account for both phenomena. An exception to this rule is of course provided by molecular dynamics simulations, where all the necessary ingredients are in principle contained in the starting, off-lattice realistic Hamiltonian. Simulations carried out for a Lennard-Jones surface [mimicking Ar(111)] have recently demonstrated the existence of PR,¹¹ but they have also suggested a new scenario for the PR transition in which the crucial role in stabilizing the DOF phase is played by the surface melting entropy of the half-filled top layer,¹² instead of just long-range step-step interactions, as suggested earlier.¹³ Hence PR may arise precisely as a result of the interplay between SM and SR, that is, between in-plane configurational and height degrees of freedom.

We have recently shown¹⁴ that a surface modeled through a domain wall in an N -state 3D Potts model will develop a SM-induced PR transition when N is large enough. Here, the logarithm of the large number of on-site states $\ln N$ plays the

role of the configurational entropy of the liquid in a real system. We also suggested, but without proof, that the PR transition in the Potts model could reproduce basically the phenomenology of rare-gas multilayers adsorbed on an attractive substrate,^{15–18} which is the physical system where an underlying PR transition has been invoked,^{19,13,9} not without some controversy.^{17,9} The SM-induced PR scenario can resolve the controversy^{14,12} and explains the experimentally observed fact that first-order PR of rare-gas solid surfaces may occur rather close in temperature to SR and SM, a possibility denied in all previous accounts of the PR transition.

It remains however to be demonstrated that this kind of N -state Potts model actually provides a good description of the layering phenomenology and of the associated layering phase diagram on a weakly attractive substrate. Building this layering phase diagram for the N -state Potts model is one of the motivations of the present work. This is done in Sec. III in a mean-field description, while the necessary definitions and a review of some known results about the three-state Potts model are provided in the preceding section, Sec. II. Another important motivation of the present work is to connect our description with the more traditional one, where the onset of PR is caused by next-nearest-neighbor interactions in SOS models. This is necessary because our approach is conceptually different. We start with a PR transition that is first order in the mean-field approximation of Sec. III and then show in Sec. IV that fluctuations can turn it continuous. A simplified description provided in Sec. V then shows that both approaches coincide in the end, with only the intimate nature of the driving mechanism of PR being different. With this simplified model we then study the various possible types of layering phase diagrams that may prove to be important in other contexts. In Sec. VI we analyze the fate of PR transitions in cases (as in fact all experimental situations) where the symmetry between the crystal and vapor phase, an ingredient implicit in both SOS and Potts model descriptions, is removed. It is found that lack of this symmetry will remove continuous PR, transforming it from a sharp transition to a gradual crossover, but that first-order PR is robust and can generally survive. Section VII contains our final conclusions.

II. THE N -STATE POTTS MODEL: SURFACE MELTING FOR $N=3$

The N -state Potts model on a simple cubic lattice in the presence of a chemical potential μ that couples to all but one state (the vapor state, chosen to be the N th) can be written as

$$H = -J \sum_{\langle i,j \rangle} \delta_{s_i, s_j} + \mu \sum_i (1 - \delta_{N, s_i}), \quad (1)$$

where $\langle i,j \rangle$ indicates first-neighbor pairs. The values of s_i range from 1 to N . For $N > 2$ this Hamiltonian is known to possess a T - μ phase diagram consisting of three bulk phases that play the role of the solid, liquid, and vapor phases of a pure substance.⁶ In fact, at low temperatures there are two possible phases. If $\mu > 0$ one obtains a (nondegenerate) ‘‘vapor’’ phase, where most of the spins s_i have the value $s_i = N$. On the other hand, if $\mu < 0$, one obtains a ‘‘solid’’ phase with a majority of spins pointing in one of the remain-

ing $N-1$ directions. This phase has degeneracy $N-1$. At higher temperature a uniform ‘‘liquid’’ phase exists in which all N states appear basically with equal probability.

We force twisted boundary conditions along one direction in 3D space, interchanging states 1 and N (state N represents the vapor, and state 1 is singled out to represent the solid). In this nonhomogeneous geometry, the system is forced to have a domain wall, and that wall is in fact our model of the crystal surface. This kind of modeling has been used before,^{20,6} although just with $N=2$ and $N=3$ within the mean-field approach only. We reproduce here for convenience the mean-field approach, following Jayanthi.⁶

Using expression (1) we write the free energy in the mean-field approach (with $\mu=0$ and up to an additive constant) as

$$F[\rho] = \sum_{i=1}^N \left[-J \sum_l \rho_l^i \rho_{l+1}^i - 2J \sum_l (\rho_l^i)^2 \right] - T \sum_l \sum_{i=1}^N \rho_l^i \ln(\rho_l^i). \quad (2)$$

Here l is the layer index perpendicular to the interface, running from minus to plus infinity, and ρ_l^i is the fraction of sites in the layer l with the value of spin equal to i . We are interested mainly in the profiles of the different ρ^i across the interface. Note that due to the symmetry of this expression all ρ_l^i with $i=2, \dots, N-1$ will be equal. Boundary conditions will be chosen to interchange the values of ρ^1 and ρ^N , thus forcing the existence of a ‘‘solid-vapor’’ interface in the system. In this way the translational symmetry upon changing $l \rightarrow l+n$ (with n an integer number) and the symmetry upon changing $l \rightarrow -l$ imply that the solutions for ρ_l^i must be invariant (upon interchanging ρ_l^1 and ρ_l^N) under the change $\rho_l \rightarrow \rho_{l_0-l}$, l_0 being an integer number. The center of symmetry is then located at $l_0/2$, and it coincides with a physical plane if l_0 is even, whereas it falls between two planes if l_0 is odd. These two different kinds of solutions will be referred to as even and odd, respectively. The possibility thus arises that upon changing temperature the interface might switch between even and odd configurations.

We minimize numerically the free energy (2) with a Monte Carlo method for different values of N . We calculate the profiles across the interface of ρ^1 and $\rho^{2,N-1} \equiv \sum_{i=2}^{N-1} \rho^i$. The physical density of the system is given by

$$\rho_l^{\text{phys}} = \rho_l^1 + \rho_l^{2,N-1}. \quad (3)$$

It is convenient to define also a ‘‘symmetric’’ density ρ^{sym} as

$$\rho_l^{\text{sym}} = \rho_l^1 + \frac{1}{2} \rho_l^{2,N-1}. \quad (4)$$

The advantage of this definition is that the mean position of the interface defined through ρ^{sym} is always (at equilibrium) at an integer or half-integer value, a property that the physical density does not have. From ρ^{sym} and ρ^{phys} we then define the average position of the interface as

$$h^{\text{phys}} = \sum_{l \geq \bar{l}} (\rho_l^{\text{phys}} - \rho_{l \rightarrow \infty}^{\text{phys}}) / (\rho_{l \rightarrow -\infty}^{\text{phys}} - \rho_{l \rightarrow \infty}^{\text{phys}}) + \bar{l}, \quad (5)$$

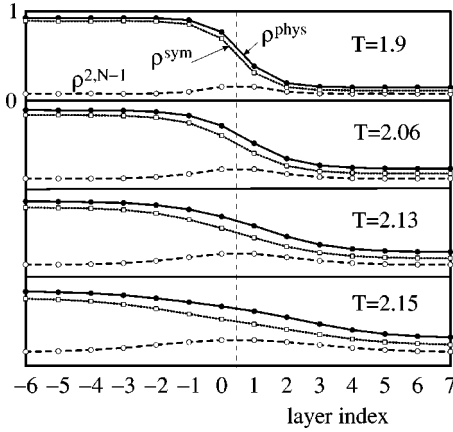


FIG. 1. Profiles of ρ^{phys} , ρ^{sym} , and $\rho^{2,N-1}$ across the interface at different temperatures, for $N=3$. The symmetry position is indicated by the dashed line.

$$h^{\text{sym}} = \sum_{l \geq \tilde{l}} (\rho_l^{\text{sym}} - \rho_{l \rightarrow \infty}^{\text{sym}}) / (\rho_{l \rightarrow -\infty}^{\text{sym}} - \rho_{l \rightarrow \infty}^{\text{sym}}) + \tilde{l}, \quad (6)$$

where \tilde{l} indicates a reference plane, well at the left of the interface (so that h^{phys} and h^{sym} are independent of \tilde{l}).

We will also refer to $\rho^{2,N-1}$ as the ‘‘amount of liquid,’’ because as explained for the bulk phase diagram, these states are mainly occupied in the liquid phase. However, the identification is not rigorous. In the solid or gas phase there is also a contribution of states 2 to $N-1$, while in the liquid phase there are some spins in states 1 and N . However, the notion is clear, and for large N the identification is reasonably precise. The total amount of liquid at the solid-vapor interface n_l can then be taken as

$$n_l = \sum_l (\rho_l^{2,N-1} - \rho_{l \rightarrow \infty}^{2,N-1}). \quad (7)$$

For $N=3$ we regained the results of Jayanthi,⁶ who found a liquid layer film wetting critically the solid-vapor interface as T approaches the triple point. The divergence of n_l is logarithmic, as expected for short-range interactions. We are interested mainly here in the first stages of surface melting, where the amount of liquid at the interface is still small. In Fig. 1 we see that in this regime the process is smooth, the interface symmetry being odd at all temperatures. We will see that the picture is different when N is increased.

III. FIRST-ORDER PR AND THE LAYERING PHASE DIAGRAM

There is an alternative to the smooth process of surface melting described in the previous section, namely layer-by-layer melting. To have a simple understanding of the problem let us consider the liquid layer at the solid-vapor interface in the Potts model as a liquid-vapor interface next to a liquid-solid one. We will characterize these two interfaces by their two mean coordinates x_1 and x_2 . Not all values of x_1 and x_2 are equally likely. The existence of the underlying lattice tells us that there will be some periodic contribution f_p to the free energy that we take to be of the form $f_p = -A[\cos(2\pi x_1) + \cos(2\pi x_2)]$. The value of A will be larger for

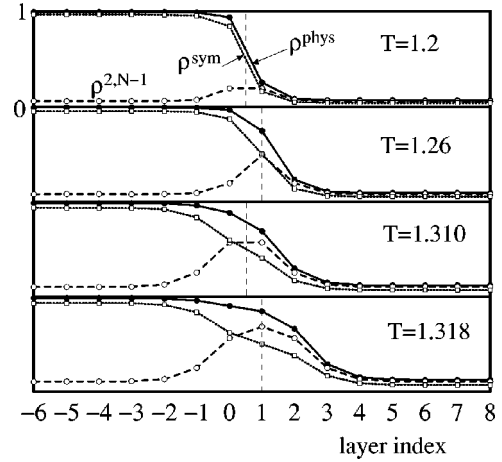


FIG. 2. Same as Fig. 1 but for $N=8$. Note the change in the symmetry position of the interface, indicated by the vertical dashed lines.

sharper interfaces, and lower for more delocalized ones. In addition, the contribution to the free energy from the coupling between x_1 and x_2 can be appropriately modeled by two additional terms. The first one is some kind of repulsion, due to conflict between the different types of order, solidlike and vaporlike, inside the thin liquid film. The second is a thermodynamic attraction, due to supercooling of the liquid film below the bulk triple point temperature. The sum of these two terms can be given the form $f_{1-2} = B \exp[-k(x_1 - x_2)] + \Delta\mu(x_1 - x_2)$, the exponential form of the repulsion being adequate for short-range microscopic interactions. When $\Delta\mu > 0$ there is an absolute minimum for $f_p + f_{1-2}$ at some finite value of $x \equiv x_1 - x_2$. By minimizing $f_p + f_{1-2}$ we obtain that x must minimize the function $f = -2A \cos(x) + B \exp(-kx) + x\Delta\mu$. As $\Delta\mu \rightarrow 0$ the value x_{\min} that minimizes this expression goes to infinity. As a function of $\Delta\mu$ as $\Delta\mu$ decreases, x_{\min} is a continuous function down to some $\Delta\mu_0$, corresponding to some typical value \tilde{x}_{\min} of x_{\min} . From here to $\Delta\mu = 0$, x_{\min} jumps discontinuously from one minimum to another of the free energy, as the most stable one moves towards $x \rightarrow \infty$. Thus in this regime the surface melting occurs in a layer-by-layer manner. The value \tilde{x}_{\min} depends on A as $\tilde{x}_{\min} \sim A^{-1/2}$. Since A increases with the sharpness of the interfaces, and that in turn increases with N in the Potts model, we can conclude that increasing N reduces the thickness of the liquid film necessary to observe layer-by-layer melting. For $N=3$ we did not find this phenomenon in the previous section precisely because the solid-liquid and liquid-vapor interfaces are in that case too wide.

For $N > 3$ the situation is different. The numerical minimization of Eq. (2) shows that layer-by-layer melting can appear starting from the first layers. Each time a new layer melts, the symmetry position of the interface changes, and there is an alternation of even and odd interfaces when temperature is increased. This sequence is illustrated in Figs. 2 and 3. The amount of liquid n_l is seen to move by steps at each temperature where the symmetry of the interface changes. Each of these changes is a first-order transition, where the free energy curves of even and odd solutions of the problem cross each other. The symmetric position h^{sym} alternates between integer and half-integer values when the tran-

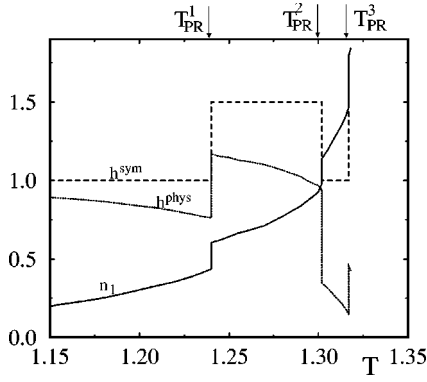


FIG. 3. Symmetrical and physical (h^{sym} and h^{phys}) positions of the interface (corresponding to the profiles of Fig. 2), and amount of liquid at the interface n_l , for $N=8$, obtained by minimizing Eq. (2).

sitions occur. The physical position h^{phys} also has jumps, however, between values that are not precisely quantized, as seen in Fig. 3. In principle an infinite sequence of transitions occurs on approaching the triple point, at temperatures T^1_{PR} , T^2_{PR} , etc., although they become progressively denser and weaker, and we are able to see only the first few.

These mean-field transitions at T^1_{PR} , T^2_{PR} , etc. are the germs of PR transitions, as it will become clear in the next sections when we present results for the model including fluctuations.²¹ First, it is instructive to consider the nature of the layering phase diagram that is obtained in the above mean-field description. Most of the experimental information on PR transitions come from layering experiments,^{15,16} where one starts with some inert substrate and deposits gas atoms, gradually growing solid layers on this substrate. We will thus work out the predictions of our model for that situation. We introduce a substrate potential that is an interaction of the substrate with the adsorbed material, by adding to the mean-field free energy (2) the terms

$$\Delta F = \sum_{i=1}^{N-1} \sum_l \left[\left(\mu - \frac{\gamma}{l^3} \right) \rho_l^i \right]. \quad (8)$$

The chemical potential has been reintroduced, and now l will be restricted to be $l \geq 1$. The l^{-3} term represents a van der Waals attraction by the substrate. For a perfectly flat solid surface this term predicts that the position of the interface l_0 is given by $l_0 \sim (\gamma/\mu)^{1/3}$.

In the presence of the substrate potential different average positions of the interface are not equivalent, and we will present the numerical result for the μ - T mean-field phase diagram of this problem. This is shown in Fig. 4 for the particular case $N=8$ and $\gamma=0.2$. The vertical axis is given as $(\gamma/\mu)^{1/3}$. In this scale the effect of the substrate potential is to produce jumps in the coverage of the film at evenly spaced intervals when $\mu \rightarrow 0$. The profiles for ρ^{phys} , ρ^{sym} , and $\rho^{2,N-1}$ in the different sectors are shown in Fig. 5. We see that below temperature T^1_{PR} , the jumps occur roughly between odd configurations of the interface (though distorted by the presence of the substrate). For $T^1_{PR} < T < T^2_{PR}$ jumps occur between even interfaces. This alternation repeats for increasing temperature. Odd and even interfaces are separated by zig-zag lines (“zippers”⁹) of first-order transitions.

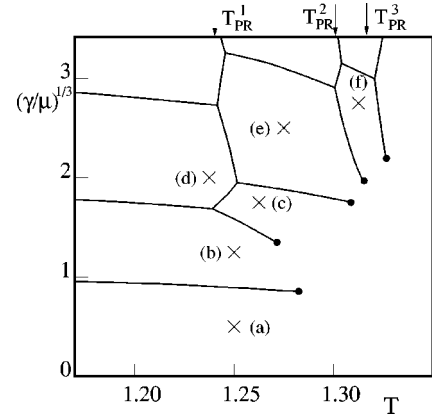


FIG. 4. The mean-field layering phase diagram, for $N=8$ and $\gamma=0.2$. For $\mu \rightarrow 0$ the zippers converge to the first-order transitions of the free-standing film (indicated by the arrows).

For $\mu \rightarrow 0$ the position of the zippers converge to the position of the first-order transitions of the free-standing film T^1_{PR} , T^2_{PR} , etc. Notice from Fig. 4 that if the substrate potential is too strong, it destroys the transitions, and the zipper is opened up, or “unzipped” from below, where the substrate potential is strongest. In this region, the first-order transition lines end in critical points, very much as is found experimentally for Ar(111) onto graphite, where this phase diagram was analyzed in detail.^{15–18}

The mean-field PR transitions T^i_{PR} become progressively weaker as the index i increases, and that is why fluctuations (in particular, roughening) will be seen to destroy the majority (or even all) of them, in the next section. In Ar(111), only one PR transition appears. However, possible experimental cases with two or more PR transitions cannot be discarded *a priori*.

IV. NUMERICAL SIMULATION OF THE FREE-STANDING INTERFACE

The original description of the PR transition characterized it as a continuous, nonuniversal phase transition.⁸ Later, it was recognized that this transition can transform to a first-order one under certain circumstances. In this work we are

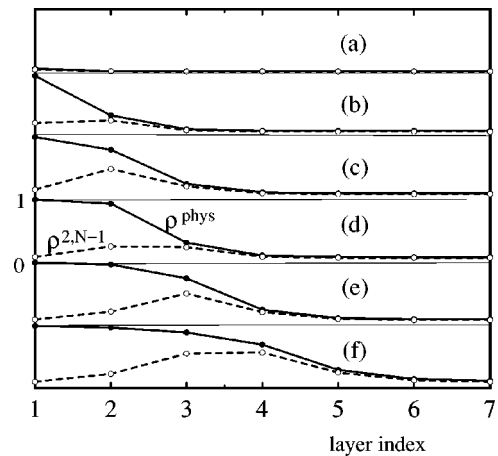


FIG. 5. Configuration of the interface at the points marked by the crosses in Fig. 4.

describing a path to PR that is opposite, in some sense, to the historical one. In the previous section we saw how a mean-field treatment of the Potts model predicts a sequence of PR transitions that are always first order. Later it will turn out that the inclusion of fluctuations can modify the nature of this sequence, leaving only a single transition (or even none) observable. Moreover, that single transition can even become continuous.

In fact, we know that liquid surfaces are always rough, due to capillary fluctuations. At high temperature and due to SM, the liquid layer at the solid-vapor interface thickens, and the free energy cost for creating steps (roughness excitations) decreases rapidly.²² This produces a roughening transition when the thickness of the liquid layer is still finite and rather small, cutting off the mean-field infinite sequence of transitions, and leaving only a small number of them. In experiments, and also in the simulations to be shown later in this section, only one PR transition is observed, indicating that an interface coated with more than a single monolayer of liquid will often (but not necessarily always) possess an excitation energy that is too small to allow the surface to remain flat.

The Hamiltonian (1) has all the necessary ingredients to obtain all these results, and we have presented Monte Carlo simulations of this model elsewhere.¹⁴ It turns out, however, that the number of Potts states necessary to obtain PR is rather large ($N \geq 50$). For smaller N the fluctuations are so strong that the interface roughens even before the first PR transition takes place. This critical value of N implies an entropy of melting ($\sim 4k_B$) that is much larger than that expected in real systems (roughly $1.7k_B$ for rare-gas solids). We then found that inclusion in the model of an additional next-nearest-neighbor interaction (i.e., a genuine parallel step-step repulsion, as in Ref. 13) strongly contributes to stabilize the flat phase. The parallel step repulsion acts to shift the roughening transition to higher temperatures, thus allowing the PR transition, which is unaffected as it involves proliferation of antiparallel steps, to appear at much lower and more reasonable values of N . To describe that physics, we add to Hamiltonian (1) the contribution

$$\Delta H = \sum_{[i,j]} J_3^{s_i, s_j} (1 - \delta_{s_i, s_j}), \quad (9)$$

where $[i,j]$ indicates third-neighbor pairs in the underlying simple cubic lattice. This interaction penalizes third neighbors in different spin states. Just by counting the energy that this term adds to different configurations of the surface, it can be seen that in fact it generates a local repulsion of parallel steps on the surface, which acts to stabilize flat phases. The energy parameter $J_3^{s_i, s_j}$ will be taken to depend on the values of the spins s_i and s_j in the following way:

$$J_3^{s_i, s_j} = J_3 \quad \text{if } s_i = 1 \text{ or } N, \text{ and } s_j = 1 \text{ or } N$$

$$J_3^{s_i, s_j} = J_3/2 \quad \text{otherwise,} \quad (10)$$

i.e., the strength of the interaction is halved if at least one of the spins is in a ‘‘liquid’’ configuration. This choice is made in order to keep the PR temperature nearly constant com-

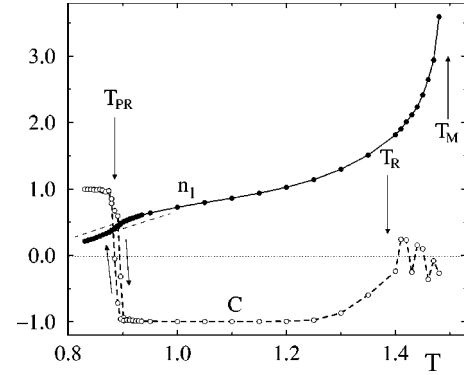


FIG. 6. Results of the numerical simulations for the complete Hamiltonian, in a system of size $40 \times 40 \times 16$, with $N=25$. From the behavior of $C \equiv \cos(2\pi h^{\text{sym}})$ we identify the PR and roughening transition temperatures T_{PR} and T_R . The bulk melting temperature T_M is signaled by the divergence of the amount of liquid at the interface n_l . The jump of this quantity at T_{PR} indicates that in this case PR is a first-order transition.

pared to the case $J_3=0$. Notice also that it still preserves the symmetry of the Hamiltonian upon interchanging states 1 and N .

We now present results obtained from a Monte Carlo study of this full model for the case of a free-standing surface. In Fig. 6 we see results for the amount of liquid n_l and the symmetrical position of the interface for $N=25$. Since in the case of a free-standing interface h^{sym} is defined up to the addition of an integer number, we define $C \equiv \cos(2\pi h^{\text{sym}})$, which should take (in the thermodynamic limit) the values $+1$ and -1 in the flat and DOF phases (where h^{sym} is respectively integer and half integer) and 0 in the rough phase, since there h^{sym} takes any real value with equal probability, and C averages to zero. This is the variable that most clearly distinguishes whether the surface is in a flat, in a DOF, or in a rough phase. Only one PR transition is observed, the evolution for $T > T_{PR}$ is smooth up to bulk melting, with a liquid film thickness that diverges logarithmically when the triple point is approached. Notice that C vanishes below the temperature where n_l diverges, i.e., there is roughening of the liquid-coated solid-vapor interface when the liquid thickness is still finite. We find that in the present case PR is first order, and the mean-field description of the previous section is qualitatively correct. In particular, we know that the system will have a layering phase diagram with only one zipper, and this coincides with the experimental situation in Ar (111). In Fig. 7 we show three snapshots of cuts across the interface, slightly below PR, slightly above PR, and slightly below bulk melting. The first two pictures show clearly the change of the symmetry position of the interface, denoting change from a flat to a DOF surface phase across the PR transition. The third picture shows a piece of a rough solid-vapor interface, coated with a liquid film about three layers thick.

Simulations with $N=10$ show the same overall behavior, except that in this case PR is continuous. In fact we see in Fig. 8 results of simulations in systems of different lateral sizes L , around the temperature where C changes sign. Here n_l has a smooth behavior, which is an indication of a continuous transition. The strongest evidence for continuous PR, however, comes from the size dependence of the interface

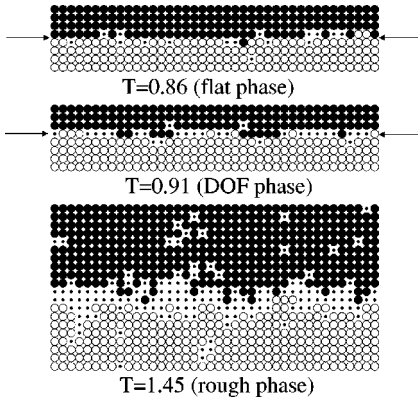


FIG. 7. Snapshots across the interface at three different temperatures ($N=25$). Circles represent spins in states 1 (filled) and N (hollow). Dots represent spins in states 2 to $N-1$ (i.e., liquid states). Note the change in the symmetry plane of the interface (indicated by the arrows) between flat and DOF phases.

thickness W^2 . From the mean (physical) position of the interface $h_{i,j}$ at each lateral position (i,j) we define W^2 as

$$W^2 \equiv \frac{1}{L^2} \sum_{i,j} (h_{i,j} - h^{\text{phys}})^2. \quad (11)$$

The interface width W^2 is infinite in rough phases in the thermodynamic limit. For finite systems it increases logarithmically with system size. The results in Fig. 8 are consistent with a logarithmic increase of W^2 exactly at the PR temperature, whereas a saturation for large sizes at temperature both above and below PR is visible. This is a strong signature of a continuous PR transition. Following divergence at PR, W^2 returns finite in the DOF phase, to diverge again and for good when the roughening temperature is approached.

The possibility of continuous PR in our model makes contact with standard descriptions of this transition. We shall explore this connection in the next section.

V. A SIMPLIFIED DESCRIPTION

In this section we elaborate on a simple description of PR in the Potts model that in our view neatly connects with the

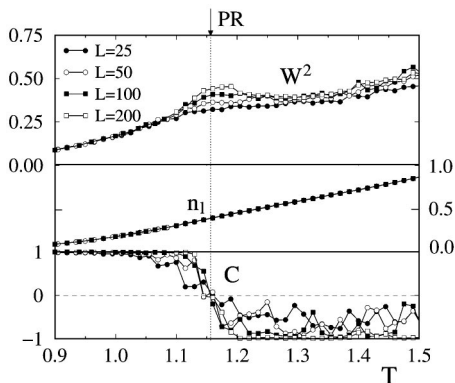


FIG. 8. Same as Fig. 6 but for $N=10$, for different lateral sizes L , as indicated. The PR transition is now continuous, as it can be seen for instance from the continuity of n_l and the logarithmic increase of W^2 with the lateral size.

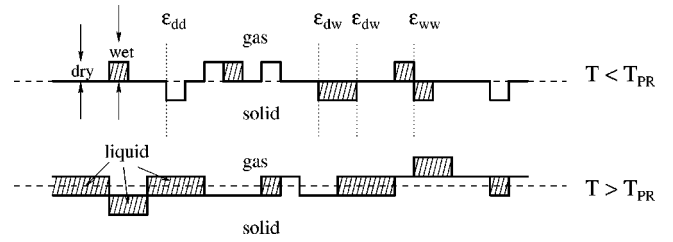


FIG. 9. Typical configuration of the interface within the simplified model of Sec. V in the flat and DOF phases. No excitations other than those shown are allowed. The energy parameters are indicated.

original description of the transition, thus emphasizing the underlying physical equivalence of PR driven by next-nearest-neighbor interactions (as in SOS models) or driven by onset of surface melting. At the end, our simple model will prove to be useful also to study some other possibilities, such as the possible existence of a first-order roughening transition in some systems.

The Potts model provides a realization of a system in which the intercell, “height” degrees of freedom (those responsible for roughening in SOS models) conspire with the intracell, “free volume” degrees of freedom (those generating a liquid layer in lattice theories of SM), to give rise to a PR transition. With a view to understand further this interplay, we will construct a model that minimally describes this situation. With this aim, we note that from the two first snapshots shown in Fig. 7, it is clear that close to the PR temperature, the amount of fluid at the interface is still very small. This is a guarantee that a reasonably good qualitative description in this temperature range can be provided by a model that allows at most one atomic layer between solid and gas to be occupied by liquid states, and that considers the vapor and solid phases as ideal (i.e., all spins in states N and 1, respectively). In our simplified description, we will define a configuration of the interface by providing (for each lateral coordinate) the position of the topmost atom of the solid (an integer number) and also distinguish whether there is or there is not a particle in a liquid configuration at the interface. A convenient way of doing that is to use integer numbers to define the position of the solid-vapor interface when there is no liquid in between, and use half-integer numbers to describe those configurations in which there is a monolayer of liquid. In this way, integer numbers represent “dry” spots at the surface, and half-integer numbers represent “wet” spots. Liquid layers of more than one layer thickness are disregarded and also the existence of liquid bubbles within solid and vapor phases.

To completely define this simplified model we must further specify the energy of each possible configuration. With the same aim used in defining “restricted” SOS models, we will allow only configurations of the surface that differ at most by one height unit between nearest-neighbor positions. Within this restriction we have then the possibility of having dry-dry, wet-wet, and dry-wet steps at the surface. They are illustrated in Fig. 9. The energies of these steps will be denoted, respectively, as ϵ_{dd} , ϵ_{ww} , and ϵ_{dw} . The absolute free energies of microscopic dry and wet interfaces will not generally be the same. We saw that in the Potts model there is an effective change in stability when these free energies cross

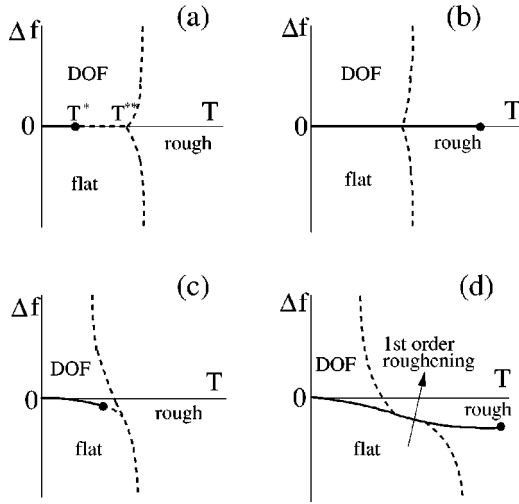


FIG. 10. The possible topologies of the phase diagram for the model described by Eq. (12) and Fig. 9. Continuous (dashed) lines indicate first-order (continuous) transitions. See the text for details.

each other. In our minimal model we will take this difference Δf to be an external parameter, and investigate the phase diagram in the plane Δf - T . Different physical possibilities will correspond to different choices of the $\Delta f(T)$ function.

The analysis of the phase behavior of this model becomes more transparent if we write its Hamiltonian in the following way,

$$H = \sum_{\langle i,j \rangle} g(h_i, h_j) + \frac{1}{2} \Delta f \sum_i \cos(2\pi h_i) - y_4 \sum_i \cos(4\pi h_i), \quad (12)$$

here it is formally assumed that h can be any real number, but we will take $y_4 \rightarrow +\infty$, thus forcing the height h_i to take only integer or half-integer values. In addition, $g(h_i, h_j)$ takes the value ε_{dw} if $|h_i - h_j| = 1/2$, and ε_{dd} (ε_{ww}) if $|h_i - h_j| = 1$ and h_i, h_j are integer (half-integer) numbers. Having written the Hamiltonian in this way, we can benefit from previous studies of the PR problem, in which a Hamiltonian very much like the previous one has been studied.

Analyzing in first place the case $\varepsilon_{dd} = \varepsilon_{ww} \equiv \varepsilon$, it is known from previous studies^{7,9} that as soon as $\Delta f \neq 0$, the minima that are higher in energy (integer or half-integer h for Δf lower or greater than 0) are irrelevant in a renormalization sense. The system has a roughening transition at some temperature that is not universal and depends on Δf . Below that temperature the surface is flat. It is pinned to an integer h value if $\Delta f < 0$, and to a half-integer value if $\Delta f > 0$. Only when $\Delta f = 0$ both minima contribute to the critical behavior of the system. In this case, if ε_{dw} is smaller than ε_{dd} , the roughening temperature will be substantially smaller (proportional to ε_{dw}) than in the case $\Delta f \neq 0$. The phase diagram is then qualitatively as depicted in Fig. 10(a). The line from $T=0$ up to $T=T^*$ at $\Delta f=0$ represents then a situation in which the surface is flat, and pinned with equal probability to an integer or half-integer height. If this line is crossed vertically, it represents a first-order PR transition. On the other hand, the dashed line between $T=T^*$ and $T=T^{**}$ is a singular prolongation of the rough phase into the flat phases. When this line is crossed by a physical $\Delta f(T)$ line it pro-

duces a continuous PR transition, which is no more than “roughening at a single temperature,” as it is sometimes defined.

Still keeping $\varepsilon_{dd} = \varepsilon_{ww}$, if ε_{dw} is increased, T^* moves to higher temperatures, and it can even penetrate in the rough phase, as indicated in Fig. 10(b). In this situation the first-order line ends within the rough phase in an Ising critical point. The first-order transition within the rough sector is between two rough phases that are still characterized by a majority of integer or half-integer values of the heights.

We turn now to a case (expected to be more realistic) where the step energy of the wet surface is smaller than that of the dry surface, namely $\varepsilon_{dd} > \varepsilon_{ww}$. For the case $\varepsilon_{dw} < \varepsilon_{ww}$ the modification of the phase diagram is only quantitative, caused by the fact that the symmetry upon changing the sign of Δf is now no longer present. Then the phase diagram of Fig. 10(a) is expected to be modified as depicted in Fig. 10(c). The limiting roughening temperatures for $\Delta f \rightarrow +\infty$ and $\Delta f \rightarrow -\infty$ are now different, being proportional to ε_{ww} and ε_{dd} , respectively. If we increase at this point ε_{dw} , a new possibility appears which is indicated in Fig. 10(d). A first-order roughening transition is possible in this case. For this transition to occur ε_{dw} has to be sufficiently large, at least larger than ε_{ww} . Although this is rather unphysical for the surface melting model we are studying, the possibility of a first-order roughening transition is an interesting by-product of our analysis, that could prove to be useful in other circumstances.

VI. ROBUSTNESS OF CONTINUOUS AND FIRST-ORDER PR TRANSITIONS

We will analyze now an important issue that is related to the possibility of realization of PR in real experimental situations. Most of the theoretical descriptions of PR given so far in the literature rely implicitly on the assumption of a symmetry between the solid and gas phase. This kind of particle-hole symmetry, which may be a good approximation in some temperature range for real systems, is of course far from exact, but its effect on the PR transition is nonetheless crucial. In this section we analyze this aspect in detail.

We already saw in the models described earlier that flat surfaces can be characterized as even and odd (namely, with a symmetry plane located at an integer or half-integer value of the z coordinate) because of the combination of the two symmetries $h \rightarrow h + n$ (with n an integer number) and $h \rightarrow -h$ of our description. The latter reflects precisely the assumed symmetry between solid and vapor phases. The lack of this symmetry allows the surface to be located at any position, and as we will presently show, it destroys the continuous PR transition.

Prasad and Weichman⁹ previously derived a phase diagram like that of Fig. 10(a) when analyzing the PR problem with renormalization techniques. They considered a Hamiltonian of the same form as Eq. (12), with $g(h_i, h_j) = K'(h_i - h_j)^2$. Near criticality, they write the Hamiltonian as

$$H = K \sum_{\langle i,j \rangle} (h_i - h_j)^2 - y_R \sum_i \cos(2\pi h_i) - u_R \sum_i \cos(4\pi h_i), \quad (13)$$

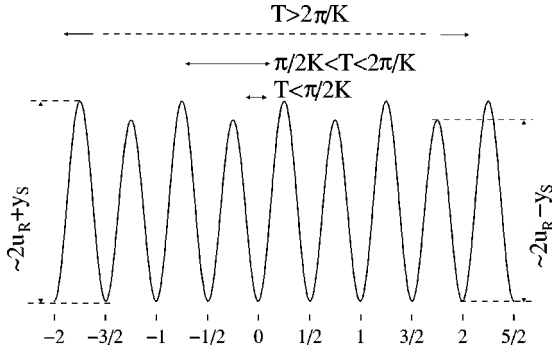


FIG. 11. The free energy of Eq. (13) with $y_R=0$, in the presence of a symmetry-breaking term $y_S \sin(2\pi h)(y_S \ll u_R)$.

where h_i takes any real value, the renormalized parameters y_R and u_R are small, and K is the renormalized stiffness.

For a general Hamiltonian $K \sum_{\langle i,j \rangle} (h_i - h_j)^2 + f(h)$, if f is an infinitesimal periodical function of h , with period λ , the roughening temperature T_r is given by $T_r = 2\pi\lambda^2/K$. Then for the Hamiltonian (13), $T_r = 2\pi/K$ if $y_R \neq 0$, and $T_r = \pi/2K$ if $y_R = 0$, since precisely at this point (and only at this point) the period of the pinning potential is halved. The singularity of the dependence of T_r on y_R explains the singular line from $T = T^*$ to $T = T^{**}$ at $\Delta f = 0$ in Fig. 10(a), at which the system is rough. A term in the potential that breaks the $h \rightarrow -h$ symmetry of the Hamiltonian can be expanded in Fourier series of $\sin(2\pi h)$. The first harmonic $\sim y_S \sin(2\pi h)$ is the only one relevant to our considerations, with y_S considered to be small with respect to u_R . In presence of this term the periodicity λ of the potential is always 1, even in the case $y_R = 0$, and the roughening temperature is always $2\pi/K$. But still, at $y_R = 0$, some physical signature must remain of the transition at $T = \pi/2K$. In fact, the first-order transition of Fig. 10(a) cannot be destroyed by an infinitesimal y_S . The potential for $y_R = 0$ is plotted in Fig. 11. For $T < \pi/2K$ the surface is trapped in one of the minima of the potential, all minima being equivalent. For $T \geq \pi/2K$, the potential is able to localize the surface only within two wells, precisely those separated by the minimum energy barrier of Fig. 11. The position of the interface is at $n + 3/4$ for the situation depicted there (corresponding to $y_S > 0$), and would be at $n + 1/4$ if y_S was negative. Only at $T = 2\pi/K$ fluctuations are strong enough to delocalize completely the surface. So we end up with the following situation. The continuous PR line from $T = T^*$ to $T = T^{**}$ in Fig. 10(a) is smeared out to a noncritical crossover by terms in the Hamiltonian that break the solid-vapor symmetry. The first-order line from $T = 0$ to $T = T^*$ remains, and the tricritical point at $T = T^*$ transforms to an Ising end point. Flat and DOF phases do not represent any more strictly integer and half-integer covered surfaces. The coverage instead passes smoothly (if $T > T^*$) from integer to half-integer values, and at $\Delta f = 0$ takes the value $n + 1/4$ or $n + 3/4$ depending on the sign of the symmetry-breaking terms. For $T < T^*$ the jump in the coverage of the surface when crossing the first-order line is finite, and vanishes like the magnetization of a 2D Ising model when $T \rightarrow T^*$.

The analysis of the present section does not invalidate our description of Sec. III, since in fact the experimental evidence indicates that the switch between flat and DOF sur-

faces is first order.¹⁵ The existence of terms breaking the solid-vapor symmetry in a real situation tells us that any potentially *continuous* PR should be experimentally searched in the form of a crossover and not as a sharp transition.

VII. CONCLUSIONS

A domain wall in the 3D N -state lattice Potts model provides a very instructive model for studying the interplay of surface melting, roughening, and preroughening (PR). We have shown that in this model PR can be driven by the additional entropy gained by the system through the appearance of an incipient liquid layer at the interface. In this way, next-nearest-neighbor height-height interactions are no longer the single ingredient leading to a PR transition, although we find that they cannot be ignored altogether. The PR transition can be continuous or first order, depending on parameters, no matter how close the roughening temperature could be. Our first-order PR transition coupled to surface melting has all the characteristics to explain qualitatively the observed phenomenology of multilayers of rare gases, as well as the microscopic grand canonical Monte Carlo simulation results. In particular we showed that the layering phase diagram, with its characteristic ‘‘zipper,’’ obtained in our model is qualitatively similar to the one obtained in experiments.

We also discussed the connection with previous accounts of PR, showing that the thermodynamics of our surface-melting-induced PR is equivalent to that of nearest-neighbor-interaction induced PR. We also analyzed other possibilities for the phase diagram of the system when parameters are changed, showing in particular that in certain cases a first-order roughening transition can take place. Also, the lack of the solid-vapor symmetry was shown to destroy a continuous PR transition, transforming the tricritical end point of first-order PR transitions to an Ising end point. This suggests that continuous PR transitions should be hard (if not impossible) to find in real experiments in surface physics. Surface melting-induced first-order preroughening should instead be the rule. It can be expected to precede roughening in surfaces where the latter occurs sufficiently close to the melting point, so that surface melting is already incipient. This disfavors those metal surfaces where roughening takes place well below melting.

A second necessary practical ingredient for the observation of PR is an efficient surface kinetics. In order to realize PR, sharp coverage changes must be readily actuated, either via exchange with the vapor, as in the case of rare-gas solids, or via surface diffusion, as it should be expected for metals and semiconductors. Surface diffusion will, once again, be all the more significant the higher the temperature, and thus the closer the melting point.

A final and more speculative point worth mentioning, even if its treatment would go beyond the present theoretical modeling, is that roughening of the solid surface is not really necessary in order to have surface melting-induced first-order PR. There are metal surfaces such as Pb(100) (Refs. 23 and 24) or Au(100) (Refs. 25 and 26), or semiconductor surfaces such as Ge(111),^{27–29} where incomplete surface melting is well documented, and which do not apparently roughen at all up to the melting point. The transition leading

these surfaces, in particular Ge(111), from the dry state to the incompletely wet states has the characteristics expected of a surface melting-induced first-order preroughening. It will be interesting to pursue further experimentally these surface transitions, with a view to ascertain if they are accompanied by a coverage jump—the hallmark of PR.

ACKNOWLEDGMENTS

This work was partly sponsored by MURST, through COFIN97 and COFIN99, by INFM, PRA LOTUS, and by EU, TMR FULPROP. Early collaboration and discussions with S. Prestipino are also acknowledged.

*Permanent address: Centro Atómico Bariloche, Bariloche, Argentina.

- ¹E. Tosatti, in *The Structure of Surfaces II*, edited by J. F. van der Veen and M. A. Van Hove (Springer, Heidelberg 1988), p. 535.
- ²J. F. van der Veen, B. Pluis, and A. W. Denier van der Gon, in *Chemistry and Physics of Solid Surfaces VII*, edited by R. Vanselow and R. F. Howe (Springer, Heidelberg, 1988), p. 455.
- ³J. D. Weeks, in *Ordering in Strongly Fluctuating Condensed Matter Systems*, edited by T. Riske (Plenum, New York, 1980), p. 293.
- ⁴A. Trayanov and E. Tosatti, *Phys. Rev. Lett.* **59**, 2207 (1987); *Phys. Rev. B* **38**, 6961 (1988).
- ⁵G. An and M. Schick, *Phys. Rev. B* **37**, 7534 (1988).
- ⁶C.S. Jayanthi, *Phys. Rev. B* **44**, 427 (1991).
- ⁷S.T. Chui and J.D. Weeks, *Phys. Rev. B* **14**, 4978 (1976).
- ⁸M. Den Nijs and K. Rommelse, *Phys. Rev. B* **40**, 4709 (1989); M. Den Nijs, *Phys. Rev. Lett.* **64**, 435 (1990).
- ⁹P.B. Weichman and A. Prasad, *Phys. Rev. Lett.* **76**, 2322 (1996); A. Prasad and P.B. Weichman, *Phys. Rev. B* **57**, 4900 (1998).
- ¹⁰S. Prestipino and E. Tosatti, *Phys. Rev. B* **59**, 3108 (1999).
- ¹¹S. Prestipino, C.S. Jayanthi, F. Ercolessi, and E. Tosatti, *Surf. Rev. Lett.* **4**, 843 (1997); C. S. Jayanthi, S. Prestipino, F. Ercolessi, and E. Tosatti, *Surf. Sci. Lett.* **460**, 503 (2000).
- ¹²F. Celestini, D. Passerone, and E. Tosatti, *Phys. Rev. Lett.* **84**, 2203 (2000).
- ¹³S. Prestipino, G. Santoro, and E. Tosatti, *Phys. Rev. Lett.* **75**, 4468 (1995).
- ¹⁴E.A. Jagla, S. Prestipino, and E. Tosatti, *Phys. Rev. Lett.* **83**, 2753 (1999).
- ¹⁵H.S. Youn and G.B. Hess, *Phys. Rev. Lett.* **64**, 918 (1990); H.S. Youn, X.F. Meng, and G.B. Hess, *Phys. Rev. B* **48**, 14 556 (1993).
- ¹⁶P. Day, M. Lysek, M. LaMadrid, and D. Goodstein, *Phys. Rev. B* **47**, 10 716 (1993).
- ¹⁷J.M. Phillips, Q.M. Zhang, and J.Z. Larese, *Phys. Rev. Lett.* **71**, 2971 (1993); J.M. Phillips and J.Z. Larese, *ibid.* **75**, 4330 (1995); *Phys. Rev. B* **56**, 15 938 (1997).
- ¹⁸F. Rieutord, R. Simon, R. Conradt, and P. Muller-Buschbaum, *Europhys. Lett.* **37**, 565 (1997).
- ¹⁹M. Den Nijs, in *Phase Transitions in Surface Films*, edited by H. Taub, G. Torzo, H. J. Lauter, and S. C. Fain (Plenum, New York, 1991), p. 247.
- ²⁰E. Burkner and D. Stauffer, *Z. Phys. B: Condens. Matter* **53**, 241 (1983); K.K. Mon, D.P. Landau, and D. Stauffer, *Phys. Rev. B* **42**, 545 (1990).
- ²¹We will keep some names (particularly PR and DOF) in the description of our model, since the thermodynamics of our problem matches exactly that of the PR problem originally studied in SOS models. However, the original meaning of these terms does not exactly apply in all details to the present description.
- ²²A.C. Levi and E. Tosatti, *Surf. Sci.* **178**, 425 (1986).
- ²³H.M. van Pinxteren and J.W.M. Frenken, *Surf. Sci.* **275**, 383 (1992).
- ²⁴F. Ercolessi, F. Di Tolla, and E. Tosatti, *Surf. Rev. Lett.* **4**, 833 (1997).
- ²⁵B.M. Ocko, D. Gibbs, K.G. Huang, D.M. Zehner, and S.G.J. Mochrie, *Phys. Rev. B* **44**, 6429 (1991).
- ²⁶G. Bilalbegovic and E. Tosatti, *Phys. Rev. B* **48**, 11 240 (1993).
- ²⁷A.W. Denier van der Gon, J.M. Gay, and J.W.M. Frenken, *Surf. Sci.* **241**, 335 (1991).
- ²⁸N. Takeuchi, A. Selloni, and E. Tosatti, *Phys. Rev. Lett.* **72**, 2227 (1994).
- ²⁹A.L. Glebov, J.P. Toennies, and S. Vollmer, *Phys. Rev. Lett.* **82**, 3300 (1999), and references therein.